Kyung Soo Lee
Joungho Han
Man Pyo Chung
Yeon Joo Jeong

Radiology Illustrated
Chest Radiology

Springer

Kyung Soo Lee • Joungho Han • Man Pyo Chung
Yeon Joo Jeong

Radiology Illustrated: Chest Radiology

Springer

Kyung Soo Lee
Department of Radiology
Samsung Medical Center
Sungkyunkwan University School of Medicine
Seoul
Korea, Republic of (South Korea)

Joungho Han
Department of Pathology
Samsung Medical Center
Sungkyunkwan University School of Medicine
Seoul
Korea, Republic of (South Korea)

Man Pyo Chung
Department of Medicine
Division of Pulmonary and Critical Care
Samsung Medical Center
Sungkyunkwan University School of Medicine
Seoul
Korea, Republic of (South Korea)

Yeon Joo Jeong
Department of Radiology
Pusan National University Hospital
Busan
Korea, Republic of (South Korea)

ISSN 2196-114X eISSN 2196-1158
ISBN 978-3-642-37095-3 ISBN 978-3-642-37096-0 (eBook)
DOI 10.1007/978-3-642-37096-0
Springer Heidelberg New York Dordrecht London

Library of Congress Control Number: 2013955297

To our spouses and children:
Kyung Sook Yi and Joo Hwang and Joo Young
Young Hee Chon and Seung Hwan and Jae Won
Seoun Min Ahn and Seung Hwan and You Seoun
Youseock Jeong and Yean and Jian

Preface

Multidetector CT images of the state-of-the-art quality are increasingly produced in thoracic imaging, and in the near future, the CT imaging is expected to substitute chest radiography especially in outpatient clinic and may be ordered as a routine admission battery examination.

In MEDLINE or other search engines, writing down several keywords regarding lung diseases with correct MeSH (Medical Subject Headings) words would promptly bring you several diseases among which you may choose correct diagnosis of pulmonary diseases in consideration of most compatible patient symptoms and signs. Likewise, we authors would like to publish a book that will guide readers to correct diagnosis, when they use correct MeSH words or keywords for describing lung lesion patterns identified on chest CT images. When readers encounter similar patterns or distribution of lung abnormalities at CT, they may need to enumerate many diseases as potential differential diagnoses. This book provides the imaging algorithms based on patterns and distributions of lung lesions and the most relevant differential diagnoses. Because all diseases could not be enlisted as potential diagnostic possibilities, we tried to enumerate as many as common diseases that appear with similar patterns and distribution. Thus, familiarity with correct glossary of terms of lung lesion description is basic prerequisite for effective and helpful reading of this book and for making a correct diagnosis seen on chest CT scans.

After enlisting the diseases showing such pattern and distribution, the text provides the key points for differential diagnosis based on clinical and imaging features and tables that outline the classic manifestations of the various diseases. For each disease, succinct description of histopathology, clinical symptoms and signs, CT–pathology correlation, and patient prognosis has been given. Thus, this book is expected to be a shepherd for imaging diagnosis of lung diseases to radiology residents, fellows for thoracic imaging, chest physicians, and general practitioners. Moreover, as many cases are illustrated with their corresponding pathology, lung pathologists may also like to read this book. Like a cherishing substance, by keeping this handy book nearby and by comparing CT images of your patients with illustrated cases shown on this book, you may narrow differential diagnoses of your cases seen in patients of your references.

In mobile web and smartphone era, such automatic diagnosis App devices are expected to be developed such that taking a photograph of representative CT image of your patient CT might bring you an easy and automatic diagnosis of the lung disease of your patient. This approach may be feasible by pattern approach using cumulative image database. We wish that this book would be a cornerstone for such App (application) in the near future.

Last but not least, we should thank Young Joo Moon for her enthusiastic editorial help and Springer people, Dr. Ute Heilmann and Ms. Lauren Kim, for encouraging us to write this precious book.

Gangnam-gu, Seoul and Seo-gu, Pusan in Korea, August 2013

Kyung Soo Lee
Joungho Han
Man Pyo Chung
Yeon Joo Jeong

Contents

Part I Focal Lung Diseases

Pattern Approach for Lung Imaging

Flowcharts “Focal involvement” and “Diffuse involvement” see following pages.

Focal Involvement

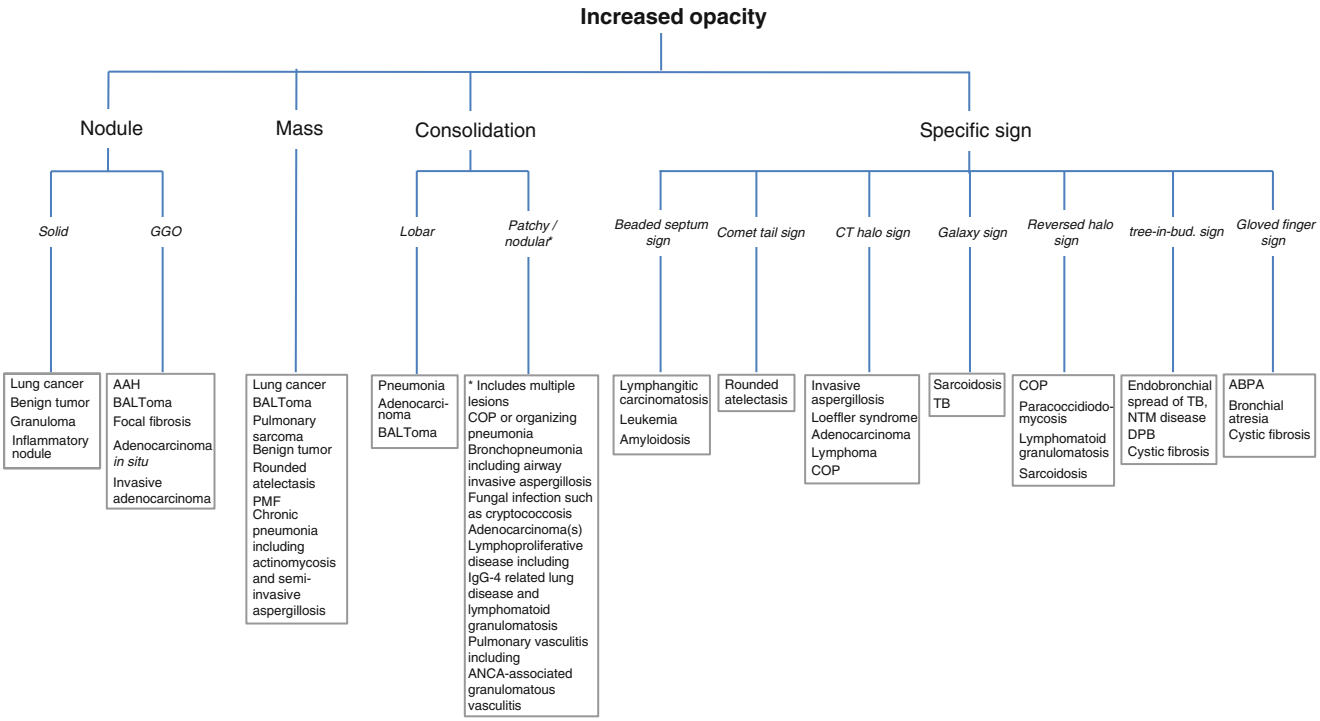

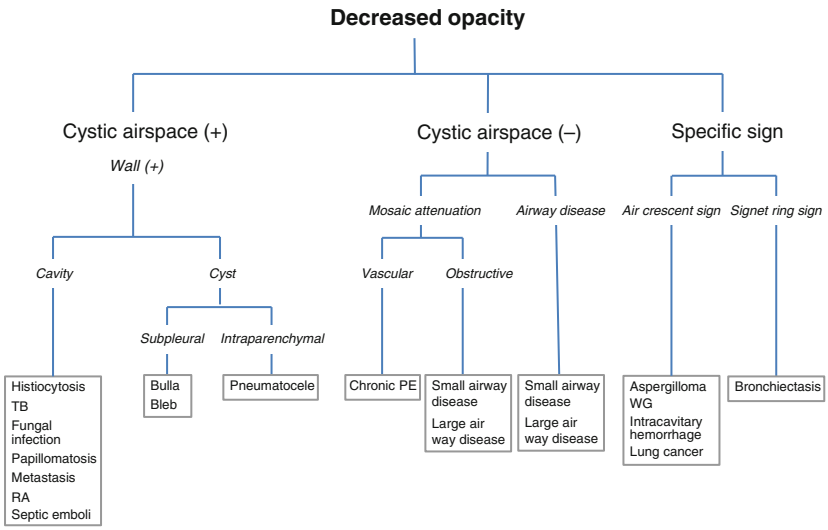

Diffuse Involvement

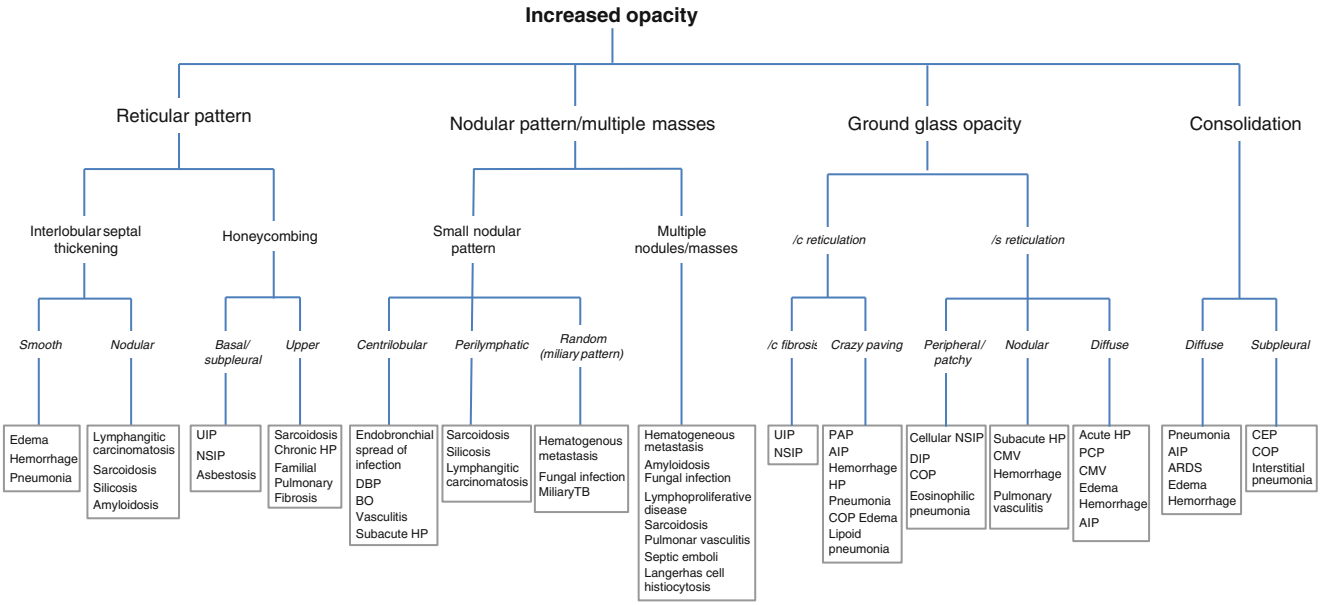

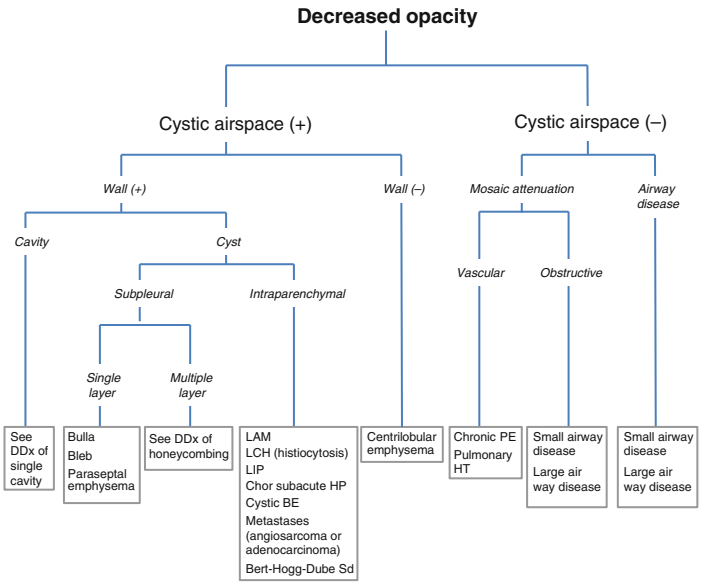

Part I

Focal Lung Diseases

Nodule

1

Solitary Pulmonary Nodule (SPN), Solid

Definition

Solitary pulmonary nodules (SPNs) are defined as focal, round, or oval areas of increased opacity in the lung with diameters of ≤3 cm [1] (Fig. 1.1). The lesion is not associated with pneumonia, atelectasis, or lymphadenopathy.

Particularly when the nodule is less than 10 mm in diameter, it may be called small nodule (Fig. 1.2). With its diameter less than 3 mm, it may be called micronodule [2].

Diseases Causing the Pattern

The most common cause is malignant tumor including *lung cancer* (Fig. 1.3), *carcinoid* (Fig. 1.4), *bronchus-associated lymphoid tissue* (*BALT*) *lymphoma* (Fig. 1.5), and a solitary metastasis to the lung. Benign tumors are *granuloma* (Fig. 1.6), *hamartoma* (Fig. 1.7), *sclerosing hemangiomas* (Fig. 1.8), *inflammatory myofibroblastic tumor* (*IMT*, *inflammatory pseudotumor*) (Fig. 1.9), rheumatoid nodule (Fig. 1.2), parasitic infection (*Paragonimus westermani*), and *nodule in antineutrophil cytoplasmic antibody* (*ANCA*)-*associated granulomatous vasculitis* (*former Wegener's granulomatosis*) (Fig. 1.10) (Table 1.1).

Fig. 1.1 A lung nodule representing lung adenocarcinoma with acinar- and papillary-predominant subtypes in a 52-year-old woman. Thin-section (2.5-mm section thickness) CT scan obtained at level of tracheal carina shows a 22-mm-sized nodule with lobulated and spiculated margin in the left upper lobe

Distribution

Likelihood ratio for malignancy in upper and middle lobe nodule is 1.22 as compared with 0.66 in lower lobe nodule [3].

Clinical Considerations

The hierarchy of radiologic and clinical likelihood ratios for malignancy includes, in decreasing rank, a cavity of 16 mm in thickness, irregular or speculated margin on CT scans, patient complaints of hemoptysis, a patient history of malignancy, patient age >70 years, nodule size of 21–30 mm in diameter, nodule growth rate of 7–464 days, an ill-defined nodule on chest radiographs, a currently smoking patient, and nodules with indeterminate calcification on CT scans [3].

K.S. Lee et al., *Radiology Illustrated: Chest Radiology*, Radiology Illustrated,
DOI 10.1007/978-3-642-37096-0_1, © Springer-Verlag Berlin Heidelberg 2014

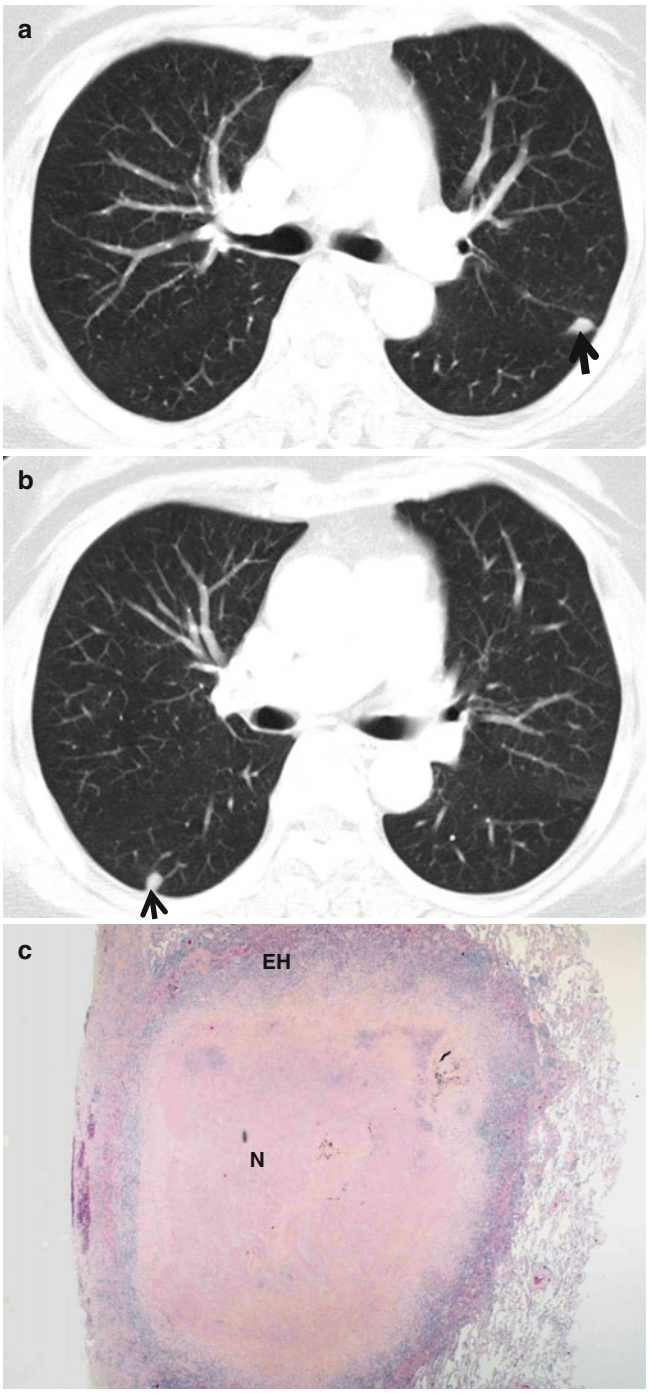

Fig. 1.2 Small nodules representing rheumatoid nodules in a 70-year-old woman with rheumatoid arthritis. (**a**, **b**) CT scans (5.0-mm section thickness) obtained at levels of main bronchi (**a**) and bronchus intermedius (**b**), respectively, show subcentimeter nodules (*arrows*) in the left upper lobe and right lower lobe. (**c**) Low-magnification (×2) photomicrograph of biopsy specimen obtained from right lower lobe nodule demonstrates central necrosis (*N*) area surrounded by a rim of epithelioid histiocytes (*EH*) and fibrous tissue

Key Points for Differential Diagnosis

1. The growth rate of small nodules should be assessed using serial volume measurements rather than diameter. Computer-aided 3D quantitative volume-measurement methods have been developed and applied clinically [4–6].
2. On multivariate analysis, lobulated or spiculated margin and the absence of a satellite nodule appear to be independently associated with malignant nodule with high odd ratio [7].
3. Diffuse, laminated, central nodular, and popcorn-like calcifications within nodules suggest benignity; on the other hand, eccentric or stippled calcifications have been described in malignant nodules [1].
4. Fat or calcification may be observed in up to 30–50 % of pulmonary hamartoma [8].
5. Evaluation based on analyses of wash-in values (>25 HU) plus morphologic features (lobulated or spiculated margin and absence of a satellite nodule) on dynamic CT appears to be the most efficient method for characterizing an SPN [9].
6. By rendering both morphologic and metabolic information, ^{18}fluorine fluorodeoxyglucose (FDG) PET–CT allows significantly better specificity than CT alone or PET alone, and both PET–CT and PET alone provide more confidence than CT alone for the characterization of SPNs [10]. But due to expensive cost and high radiation dose, it may be selectively used to characterize SPNs when dynamic CT shows inconsistent results between morphologic and hemodynamic nodule characteristics [1].
7. Specifically for small nodules less than 10 mm in diameter, serial volume measurements of nodules are regarded as the most reliable technique for their characterization [1].

Lung Cancer (Solid Adenocarcinoma)

Pathology and Pathogenesis

Adenocarcinoma is the most common histologic type of lung cancer in many countries. Adenocarcinoma is a malignant epithelial tumor with glandular differentiation or mucin production, showing lepidic, acinar, papillary, solid, and micropapillary pattern or a mixture of these patterns [11] (Figs. 1.1 and 1.3).

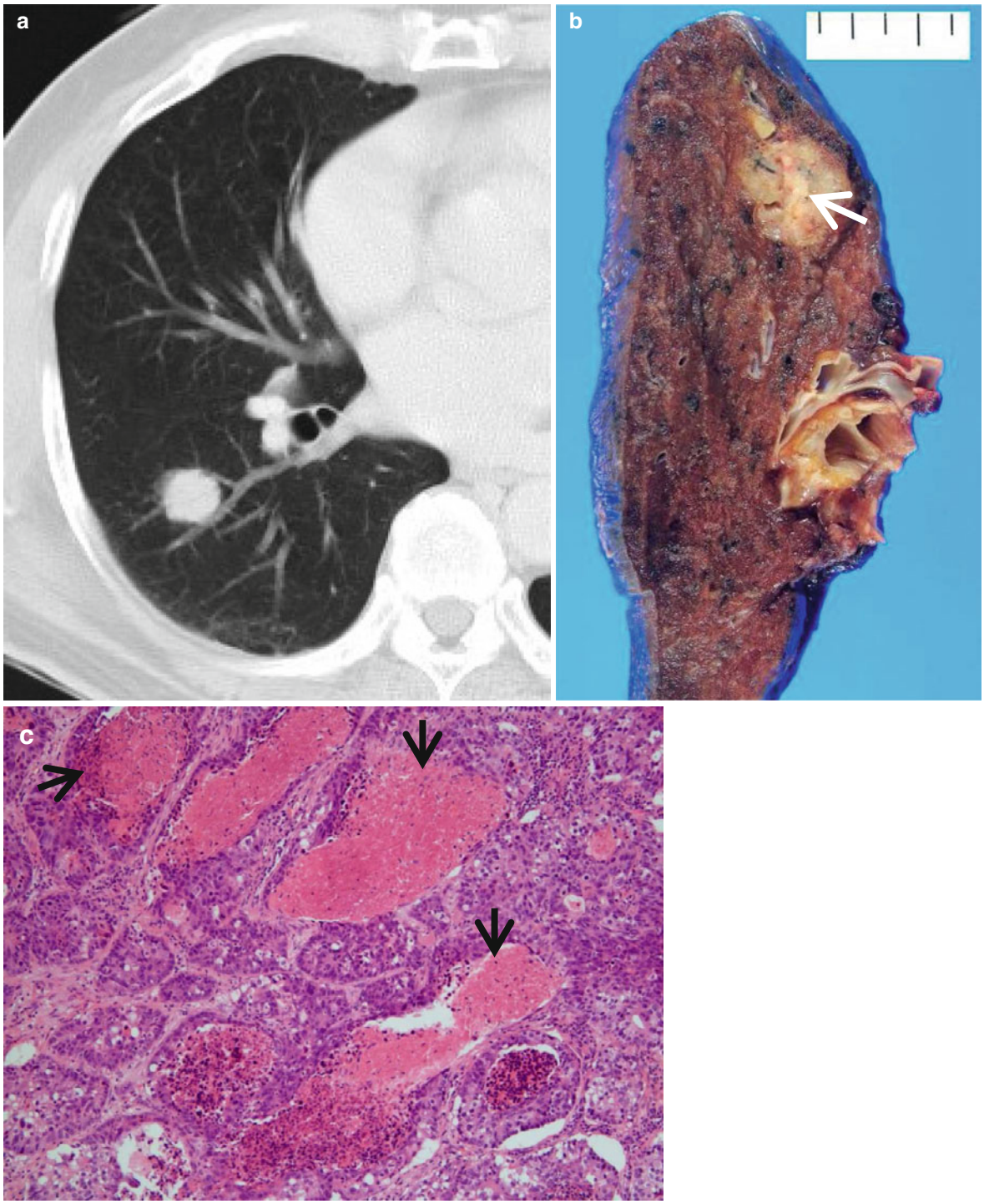

Fig. 1.3 High-grade lung adenocarcinoma simulating a metastatic nodule from a colon cancer in a 65-year-old man. (**a**) CT scan (5.0-mm section thickness) obtained at level of truncus basalis shows a 21-mm-sized nodule in superior segment of the right lower lobe. (**b**) Gross pathologic specimen demonstrates a yellowish-gray round nodule with yellow necrotic spots (*arrow*). (**c**) High-magnification (×200) photomicrograph discloses high-grade, enteric-type lung adenocarcinoma showing glandular structures with multifocal dirty necrosis (*arrows*) simulating metastatic colon adenocarcinoma

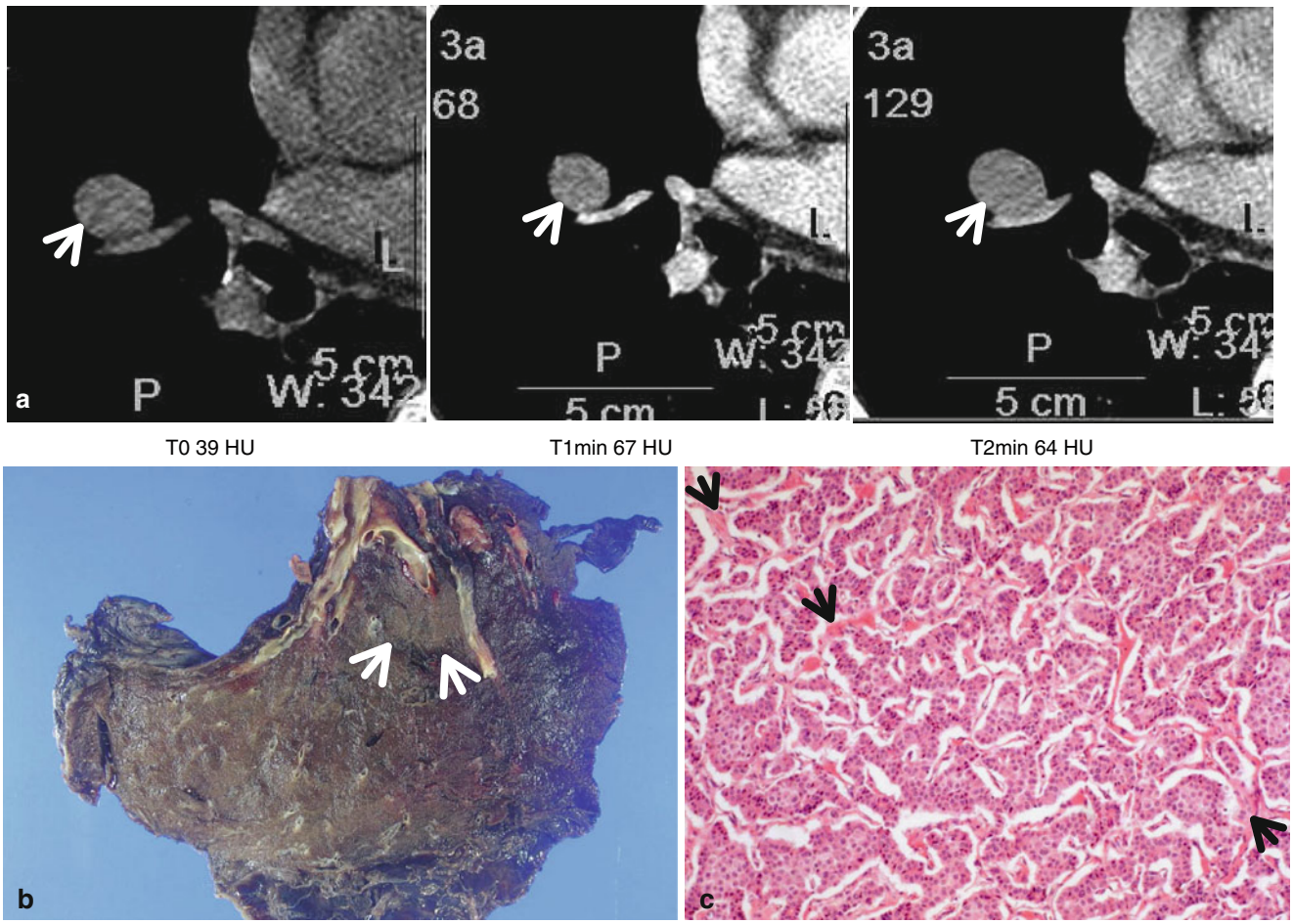

Fig. 1.4 Typical carcinoid tumor showing high and early enhancement in a 58-year-old man. (**a**) Dynamic CT scans obtained at level of right middle lobar bronchus takeoff show an 18-mm-sized well-defined nodule (*arrows*) in the right middle lobe. Nodule depicts high enhancement (39 HU, 67 HU, and 64 HU; before, at 1 min, and at 2 min after contrast-medium injection, respectively). (**b**) Gross pathologic specimen demonstrates a well-defined nodule (*arrows*) in the right middle lobe adjacent to the segmental bronchus. (**c**) High-magnification (×100) photomicrograph of right lower lobectomy specimen discloses neoplastic cells grouped in small nests separated by numerous thin-walled vascular stroma (*arrows*)

Symptoms and Signs

Patients with lung cancer presenting with an SPN are usually asymptomatic. Physical examination shows no specific abnormality. In most cases, the SPN is detected by routine chest imaging.

CT Findings

The characteristic CT finding of solid adenocarcinoma consists of a solitary nodule or mass with a lobulated or spiculated margin. On multivariate analysis, lobulated or spiculated margin and the absence of a satellite nodule appear to be independently associated with malignant nodule with high odd ratio [7]. The nodules enhance following intravenous administration of contrast medium. The enhancement of >25 HU plus morphologic malignant features on dynamic CT appears to be the most efficient method for characterizing a malignant SPN [9].

CT–Pathology Comparisons

The histopathologic correlation of spiculated margin is variable and may correspond to the strands of fibrous tissue that extend from the tumor margin into the lung, to the direct infiltration of tumor into the adjacent parenchyma, to the

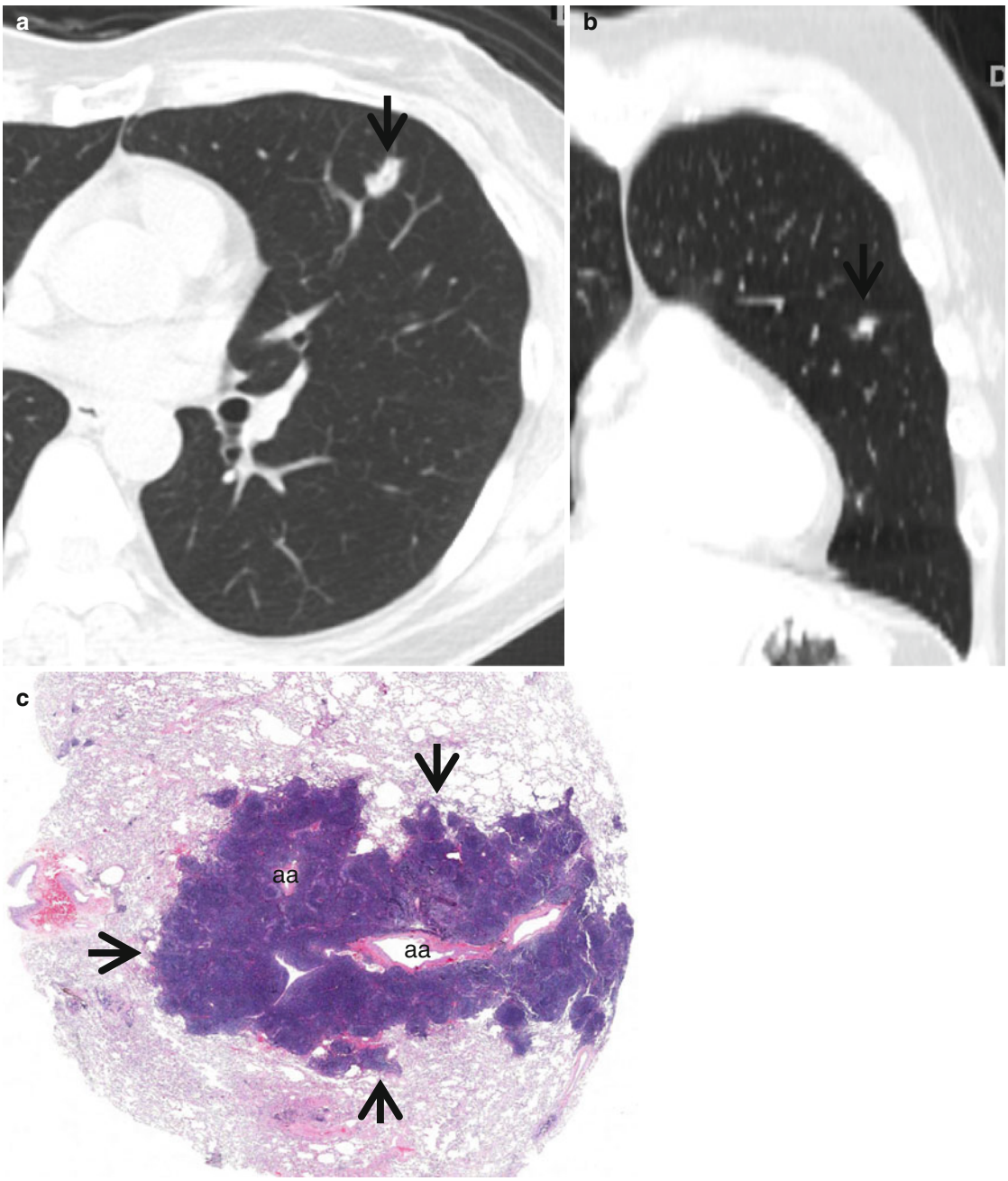

Fig. 1.5 Bronchus-associated lymphoid tissue (BALT) lymphoma in a 51-year-old woman. (**a**, **b**) Transverse (**a**, 2.5-mm section thickness) and coronal reformatted (**b**) CT scans, respectively, show a 13-mm-sized polygonal nodule (*arrows*) in lingular division of the left upper lobe. Lesion has internal CT air-bronchogram sign. (**c**) Low-magnification (×2) photomicrograph of biopsy specimen obtained from left upper lobe nodule demonstrates lymphoepithelial lesions (*arrows*) surrounding the pulmonary arteries (*aa*) and their accompanying bronchi (lumina have been compressed and collapsed)

small foci of parenchymal collapse as a result of bronchiolar obstruction by the expanding tumor, or to the spread of tumor cells into the lymphatic channels and interstitial tissue of adjacent vessels, airways, or the interlobular septa [12]. The enhancement of nodules presumably reflects the vascular stroma of the tumor [13].

Patient Prognosis

In solitary adenocarcinomas with part-solid and solid nodule, the prognosis depends on nodal and distant metastasis. Solid tumors exhibit more malignant behavior and have a poorer prognosis than part-solid tumors [14].

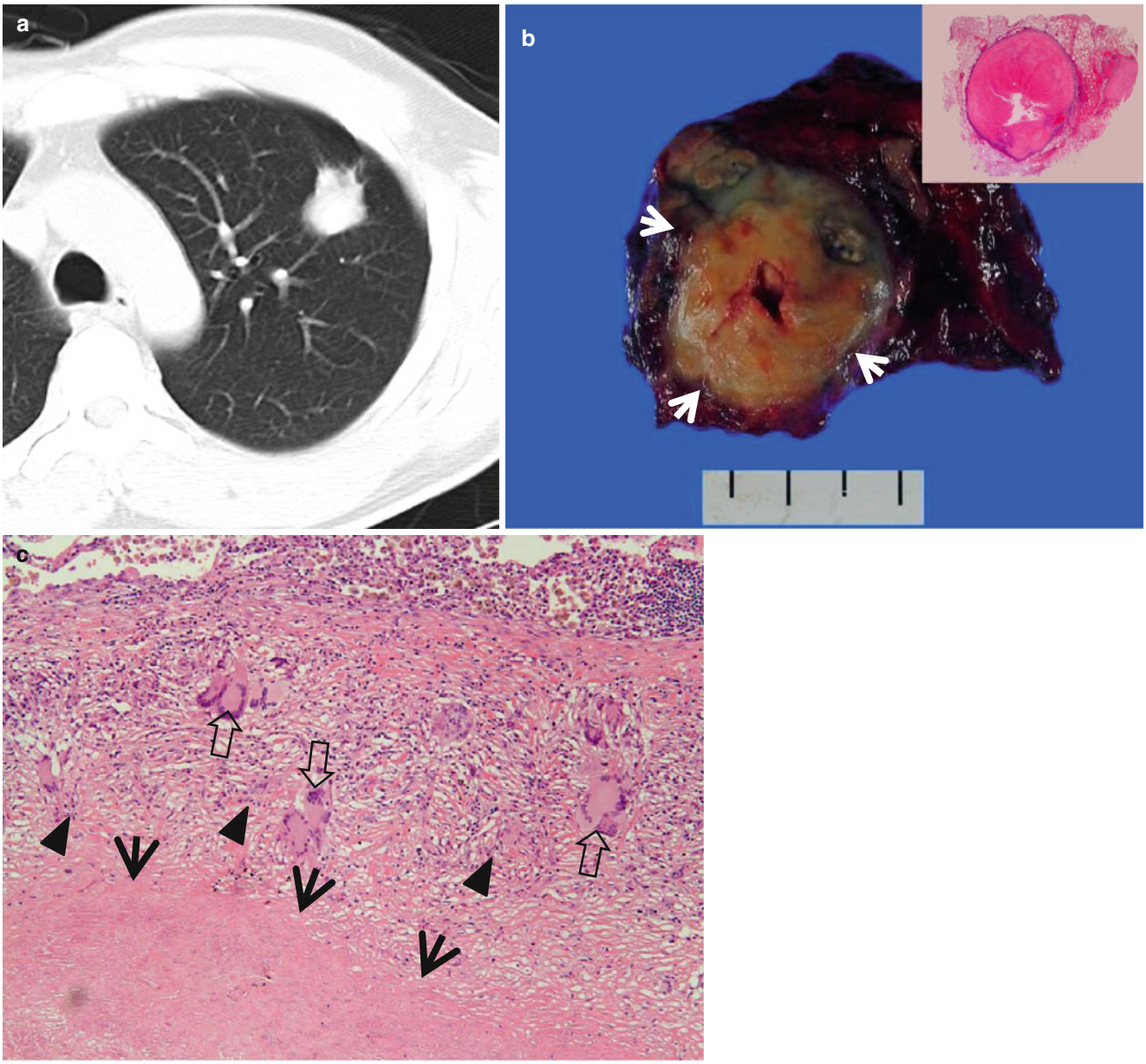

Fig. 1.6 Tuberculoma in a 47-year-old woman. (**a**) CT scan (5.0-mm section thickness) obtained at level of aortic arch shows a 27-mm-sized nodule in anterior segment of the left upper lobe. (**b**) Gross pathologic specimen demonstrates a well-defined round nodule (*arrows*). *Inset*: central caseation necrosis and peripheral epithelioid histiocytes, multinuclear giant cells, and collagenous tissue. (**c**) High-magnification (×100) photomicrograph discloses a focus of a necrotic lung (*arrows*) surrounded by a layer of epithelioid histiocytes (*arrowheads*) and scattered giant cells (*open arrows*). Numerous lymphocytes and collagenous tissues are seen adjacent to granulomatous inflammation

Carcinoid or Atypical Carcinoid

Pathology and Pathogenesis

Carcinoids are slow-growing neuroendocrine tumors characterized by their growth patterns (organoid, trabecular, insular, palisading, ribbon, rosette-like arrangements). They consist of typical carcinoids and atypical carcinoids according to mitotic count or presence of necrosis. Carcinoid is a distinct disease entity, discriminated from other pulmonary neuroendocrine tumors such as large cell neuroendocrine carcinoma or small cell carcinoma [15] (Fig. 1.4).

Symptoms and Signs

Typical carcinoid may be accompanied with hormone-related manifestations. Fewer than 5 % have the carcinoid syndrome (cutaneous flushing, bronchospasm, diarrhea). Cushing's syndrome can also occur. Atypical carcinoid, one

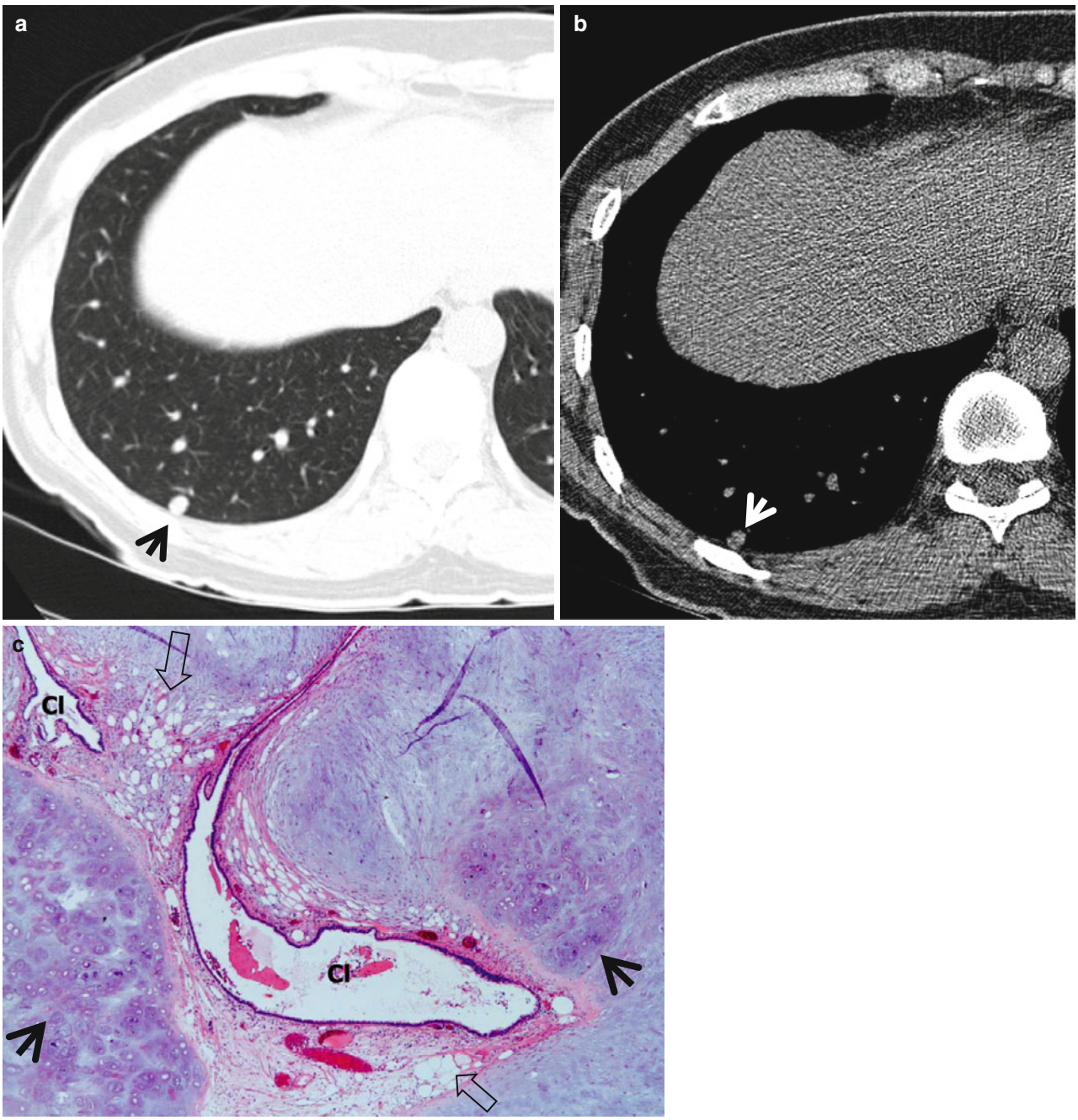

Fig. 1.7 Chondroid hamartoma in a 40-year-old woman. (**a**, **b**) Lung (**a**) and mediastinal (**b**) window images of CT scan (5.0-mm section thickness) obtained at level of lover dome show an 8-mm-sized well-defined nodule (*arrows*) in posterior basal segment of the right lower lobe. Please note fat and calcification attenuation areas within nodule. (**c**) Low-magnification (×10) photomicrograph of wedge resection from the right lower lobe demonstrates islands of mature chondroid (*arrows*) and adipocytic (*open arrows*) tissues. Also note entrapped bronchiolar epithelial cleft (*Cl*) within lesion

on the contrary, may cause lymph node and distant metastasis in half of the cases.

CT Findings

The most common imaging finding of carcinoid is a lung nodule or a mass. The CT features of a peripheral carcinoid presenting as SPN include a lobulated nodule of high attenuation on contrast-enhanced CT; nodule that densely enhances with IV contrast-medium administration; the presence of calcification (approximately 30 % of cases have calcification on CT) (Fig. 1.4); subsegmental airway involvement on thin-section analysis; and nodules associated with distal hyperlucency, bronchiectasis, or atelectasis [16]. Typical carcinoid tends to be smaller (average diameter 2 cm) than atypical

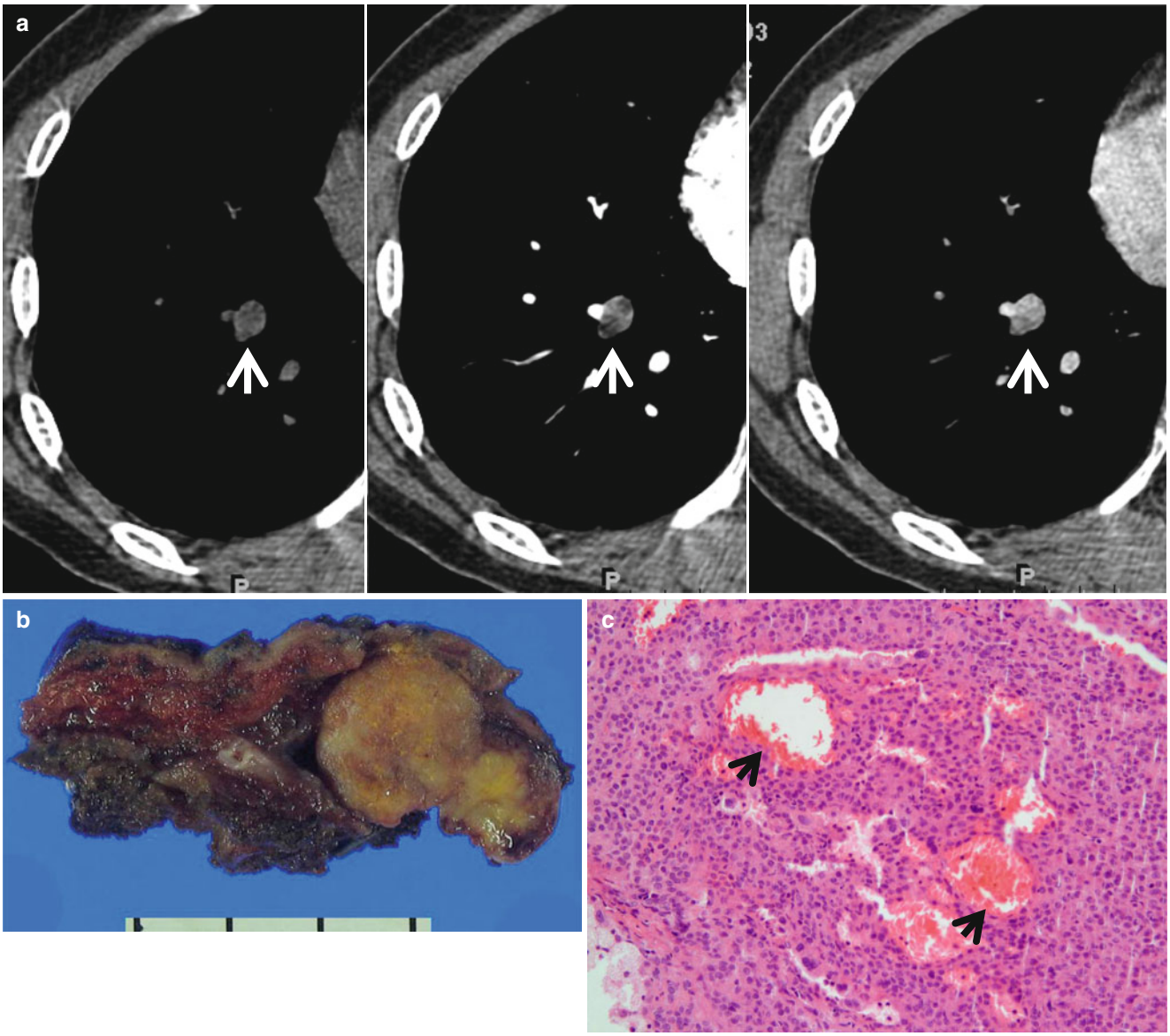

Fig. 1.8 Sclerosing pneumocytoma (hemangiomas) showing high and early enhancement in a 50-year-old woman. (**a**) Dynamic CT scans obtained at level of suprahepatic inferior vena cava (IVC) show a 16-mm-sized well-defined nodule (*arrows*) in the right lower lobe. Nodule depicts high enhancement (19 HU, 38 HU, and 69 HU; before, at 1 min, and at 2 min after contrast-medium injection, respectively). (**b**) Gross pathologic specimen obtained with wedge tumor resection demonstrates a well-defined yellowish round nodule. (**c**) High-magnification (×200) photomicrograph discloses solid growth of polygonal cells with internal hemorrhagic spaces (*arrows*)

carcinoid (average diameter 4 cm) [17]. Secondary effects on distal lung parenchyma such as distal hyperlucency are uncommon in atypical carcinoids.

CT–Pathology Comparisons

The neoplastic cells of carcinoids are grouped in small nests or trabeculae separated by a prominent vascular stroma (Fig. 1.4). Because of their vascular stroma, most carcinoids show marked enhancement following intravenous administration of contrast [18]. Segmental or lobar atelectasis, obstructive pneumonitis, and segmental oligemia are related to complete or partial obstruction of airway.

Patient Prognosis

Since typical carcinoids are extremely slow growing, the long-term prognosis is excellent if completely resected.

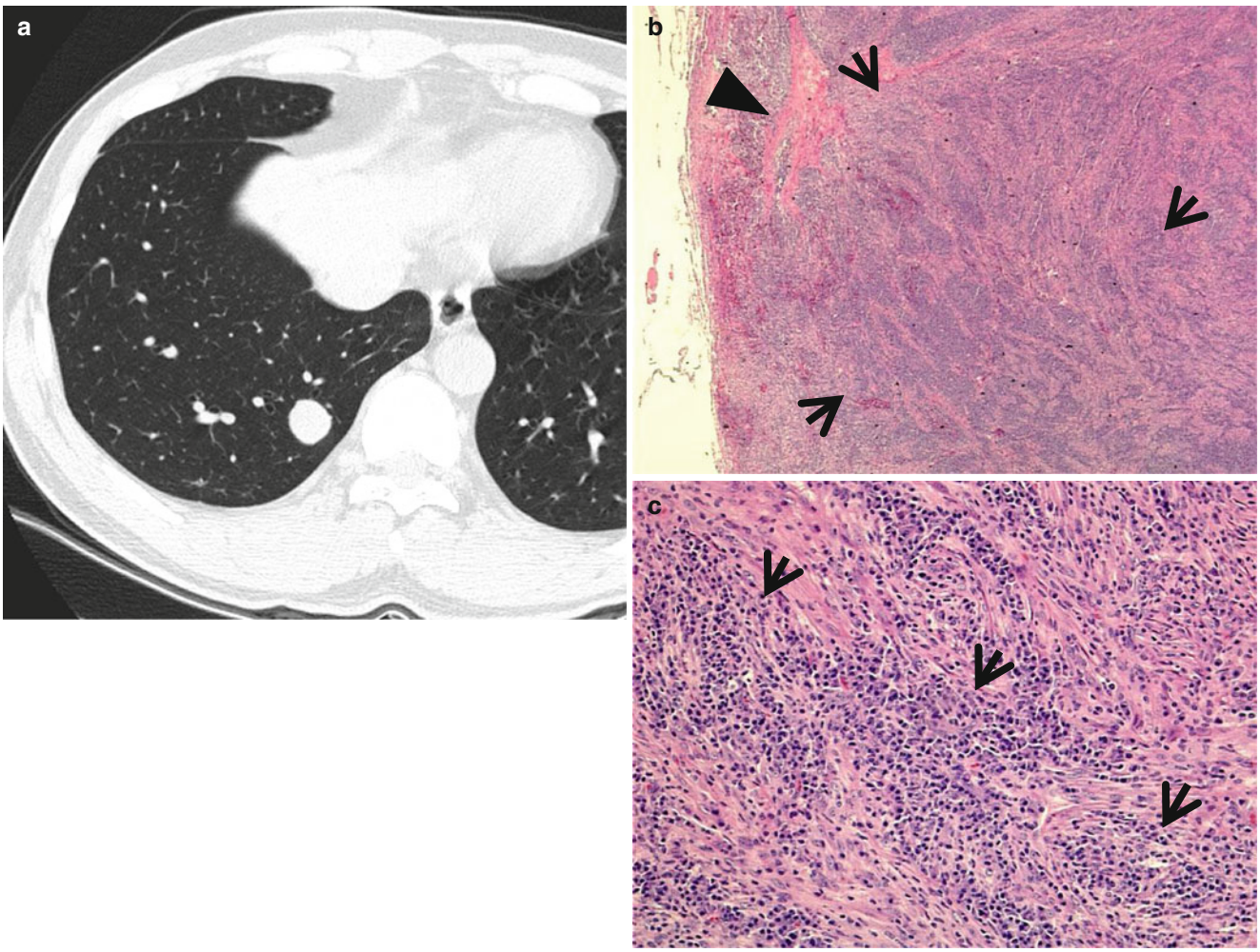

Fig. 1.9 Inflammatory myofibroblastic tumor in a 29-year-old man. (**a**) Thin-section (2.5-mm section thickness) CT scan obtained at level of suprahepatic inferior vena cava (IVC) shows a 19-mm-sized well-defined nodule in the right lower lobe. (**b**) Low-magnification (×2) photomicrograph of wedge resection of tumor from the right lower lobe demonstrates areas of inflammatory cell infiltration (*arrows*; mainly composed of plasma cells) and fibrosis (*arrowhead*). (**c**) High-magnification (×100) photomicrograph discloses fascicular spindle cell proliferation and admixed areas of lymphocytes and plasma cells (*arrows*)

However, all carcinoids are malignant although indolent. Nodal involvement clearly affects survival [19]. The 5-year survival of patients with atypical carcinoids is only 57 %.

BALT Lymphoma

Pathology and Pathogenesis

Pulmonary marginal zone B-cell lymphoma of bronchus-associated lymphoid tissue (BALT) is an extranodal lymphoma, which is thought to arise in acquired MALT secondary to inflammatory or autoimmune processes. The neoplastic cells infiltrate the bronchiolar epithelium, forming lymphoepithelial lesion [20] (Fig. 1.5).

Symptoms and Signs

BALT lymphoma of SPN rarely causes pulmonary symptoms. Weight loss and night sweating may be found. Extrapulmonary symptoms and signs of connective tissue diseases such as Sjögren's syndrome, systemic lupus erythematosus, and rheumatoid arthritis may occur.

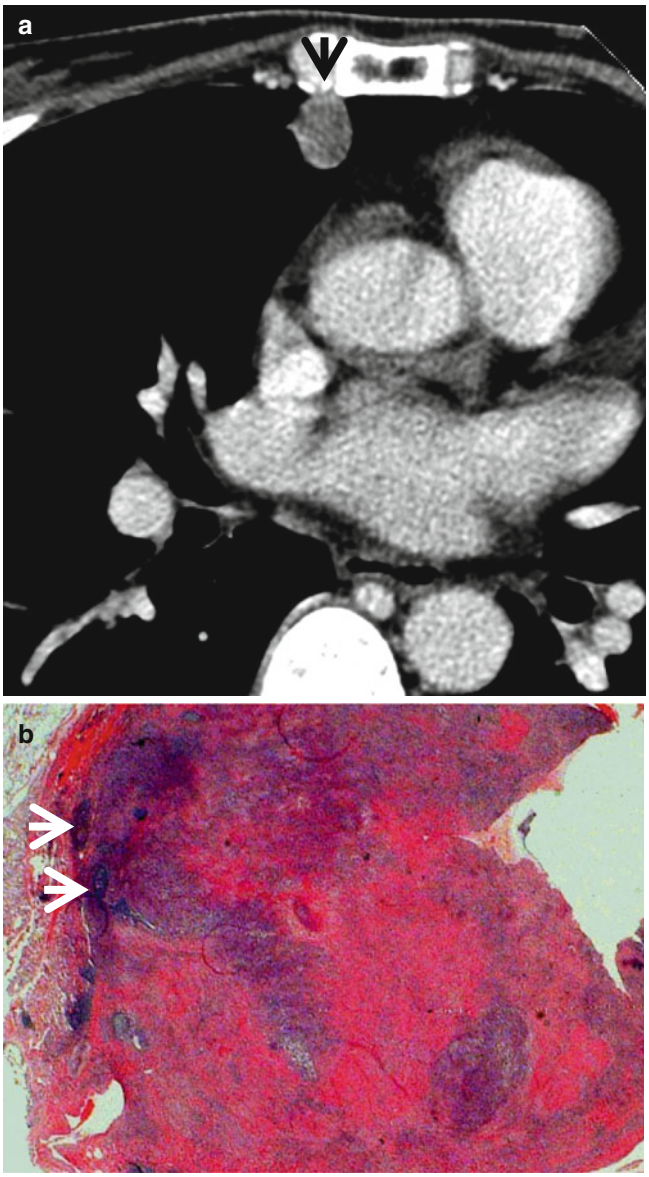

Fig. 1.10 ANCA (antineutrophil cytoplasmic antibody)-associated granulomatous vasculitis (former Wegener's granulomatosis) manifesting as a solitary pulmonary nodule in a 51-year-old woman. (**a**) Mediastinal window image of CT scan (5.0-mm section thickness) obtained at level of the right middle lobar bronchus shows a 13-mm-sized nodule (*arrow*) in the right middle lobe. (**b**) Low-magnification (×40) photomicrograph of wedge resection of tumor from the right middle lobe demonstrates basophilic inflammatory nodule containing geographic necrotic areas (*arrows*)

CT Findings

Typical CT findings of BALT lymphoma include solitary (Fig. 1.5) or multifocal nodules or masses and areas of airspace consolidation with an air bronchogram [20, 21]. Less common findings include ground-glass opacity (GGO) lesion, interlobular septal thickening, centrilobular nodules, and bronchial wall thickening and pleural effusion.

Table 1.1 Common diseases manifesting as solitary pulmonary nodule

Disease	Key points for differential diagnosis
Malignant nodule	
Lung cancer	Wash-in values of >25 HU, lobulated or spiculated margin, and absence of a satellite nodule
Carcinoid	Lobulated nodule with dense enhancement
BALT lymphoma	Consolidation or nodules with air bronchograms
Solitary metastasis	
Benign nodule	
Granuloma	No or little enhancement, satellite nodules
Hamartoma	Focal areas of fat or calcification, septal or cleft-like enhancement
Sclerosing hemangioma	Subpleural homogeneous mass, rapid and strong enhancement
Inflammatory myofibroblastic tumor	
Rheumatoid nodule	
Parasitic infection (PW)	Cavitary nodules or masses in the subpleural or subfissural areas
ANCA-associated granulomatous vasculitis	Multiple, bilateral, subpleural nodules or masses

Note: *HU* Hounsfield unit, *BALT* bronchus-associated lymphoid tissue, *PW* *Paragonimus westermani*, *ANCA* antineutrophil cytoplasmic antibody

CT–Pathology Comparisons

CT findings of BALT lymphoma showing solitary or multifocal nodules or masses and areas of airspace consolidation are related to proliferation of tumor cells within the interstitium such that the alveolar airspaces and transitional airways are obliterated [22] (Fig. 1.5). Because the bronchi and membranous bronchioles tend to be unaffected, an air bronchogram is common. Interlobular septal thickening, centrilobular nodules, and bronchial wall thickening on CT images are related to perilymphatic interstitial infiltration of tumor cells.

Patient Prognosis

BALT lymphoma shows the indolent clinical course. The estimated 5- and 10-year overall survival rates have been reported to be 90 and 72 %, respectively [23]. Age and performance status are the prognostic factors.